Mon. Not. R. Astron. Soc. **000**, 000–000 (0000) Printed 22 October 2018 (MN LATEX style file v2.2)

Xspect, estimation of the angular power spectrum by computing cross-power spectra with analytical error bars

M. Tristram, J. F. Macías-Pérez, C. Renault, D. Santos
Laboratoire de Physique Subatomique et de Cosmologie, 53 Avenue des Martyrs, 38026 Grenoble Cedex, France

22 October 2018

ABSTRACT

We present Xspect, a method to obtain estimates of the angular power spectrum of the Cosmic Microwave Background (CMB) temperature anisotropies including analytical error bars developed for the ARCHEOPS experiment. Cross-power spectra are computed from a set of maps and each of them is in itself an unbiased estimate of the power spectrum as long as the detector noises are uncorrelated. Then, the cross-power spectra are combined into a final temperature power spectrum with error bars analytically derived from the cross-correlation matrix.

This method presents three main useful properties : (1) no estimation of the noise power spectrum is needed, (2) complex weighting schemes including sky covering and map noise properties can be easily taken into account, and corrected for, for each input map, (3) error bars are quickly computed analytically from the data themselves with no Monte-Carlo simulations involved. Xspect also permits the study of common fluctuations between maps from different sky surveys such as CMB, Sunyaev-Zel'dovich effect or mass fluctuations from weak lensing observations.

Key words: – cosmic microwave background – Cosmology: observations – Methods: data analysis

1 INTRODUCTION

The measurement of the angular power spectrum of the CMB anisotropies, C_ℓs, has become one of the most important tools in modern cosmology. As long as they remain in the linear regime, the fluctuations predicted by most inflationary scenarii (Hu et al. 1997; Linde et al. 1999; Liddle & Lyth 2000) lead to Gaussian anisotropies on the CMB. Thus the angular power spectra in temperature and polarization contain all the cosmological information on the CMB sky. Cosmological parameters and other physical quantities of interest in the early Universe can be directly derived from them. In parallel to the explosion of CMB datasets both in size and quality (WMAP (Bennett et al. 2003), ARCHEOPS (Benoît et al. 2003), BOOMERANG (Ruhl et al. 2003), MAXIMA (Jaffe et al. 2003), DASI (Halverson et al. 2002), VSA (Grainge et al. 2003), CBI (Sievers et al. 2003), ACBAR (Kuo et al. 2004)), fast codes have been developed to estimate the CMB angular power spectrum (CMBFAST (Seljak & Zaldarriaga 1996; Zaldarriaga et al. 1998; Zaldarriaga & Seljak 2000), CAMB (Lewis et al. 2000)) allowing us to compare fast and efficiently theory and observations using powerful statistical tests (CMBEASY (Doran 2003), COSMOMC (Lewis & Bridle 2002), (Douspis et al. 2001)). Furthermore, huge efforts are undertaken to ease the estimation of the angular power spectrum from input CMB maps in order to cope with larger, deeper and more complex sky surveys in a reasonable amount of computing time.

Excluding very specific methods – for example those which are under study for the PLANCK satellite mission and which take advantage of the PLANCK ring scanning strategy (van Leeuwen et al. 2002; Challinor et al. 2002; Ansari et al. 2003) – most CMB power spectrum estimators can be grouped into two categories : maximum likelihood and 'pseudo'-C_ℓ estimators. A complete review and comparison between the two methods can be found in Efstathiou 2004, here we just discuss the key points of each of them.

Maximum likelihood methods for temperature anisotropies (Bond et al. 1998; Tegmark 1997; Borrill 1999a) are based on the maximization of the quadratic likelihood. The method estimates the sky angular power spectrum from the angular correlation function of the data. Error bars for the power spectrum are generally computed directly from the likelihood function which is either fully sampled in the range of interest or approximated by a quadratic form. Dealing with an inhomogeneous coverage of the sky involves a great computational complexity $\mathcal{O}\left(N_{pix}^3\right)$, where N_{pix} is the number of pixels of the input map. Therefore, these methods are very CPU

time consuming for current large datasets like WMAP and probably not well adapted (Borrill 1999b) for future satellite missions like PLANCK which will produce maps of the sky of more than $N_{pix} = 5 \times 10^7$ pixels. A generalization of these methods to the analysis of CMB polarization is discussed in Tegmark & de Oliveira-Costa 2001.

Alternatively, the so-called 'pseudo-C_ℓ's estimators compute directly the *'pseudo'* angular power spectrum from the data. Then, they correct it for the sky coverage, beam smoothing, data filtering, pixel weighting and noise biases. A comprehensive description of this method was first given by Peebles 1973 and an application to the angular clustering of galaxies can be found in Peebles & Hauser 1974. More recently, several approaches to this method have been developed. Among them, SPICE (Szapudi et al. 2001) and its extension to polarization (Chon et al. 2004) compute in the real space first the correlation function to correct for the sky coverage bias and then the power spectrum from the latter. A pseudo-C_ℓ estimator in the spherical harmonic space applied to CMB experiments is given in Wandelt et al. 2001 and Hivon et al. 2002 (MASTER). They computes directly the power spectrum before correct it for the different biases. An approach applied to apodised regions of the sky is presented in Hansen et al. 2002 and extended to polarization in Hansen & Górski 2003. These estimators can be evaluated using fast spherical harmonic transforms $\mathcal{O}\left(N_{pix}^{3/2}\right)$ and therefore provide fast and accurate estimates of the C_ℓs. However, they require an accurate knowledge of the instrumental setup and noise in order to correct them for the biases discussed previously. In fact, they use an estimation of the power spectrum of the noise in the map, generally computed via Monte-Carlo simulations, which is subtracted from the original power spectrum. This is also used to estimate the error bars in the power spectrum by calculating the variance of the C_ℓs over the set of simulations.

In this paper, we describe a method to estimate the C_ℓs by computing the cross-power spectra between a collection of input maps coming either from multiple detectors of the same experiment or from different instruments. The 'pseudo' cross-power spectra are explicitly corrected for incomplete sky coverage, beam smoothing, filtering and pixelization. Assuming no correlation between the noise contribution from two different maps, each of the corrected cross-power spectra is an unbiased estimate of the C_ℓs. Analytical error bars are derived for each of them. The cross-power spectra, that do not include the classical *auto*-power spectra, are then combined using a Gaussian approximation of the likelihood function. In the same way, we can also compute the estimate of the common angular power spectrum, C_ℓ^{common}, of sky maps from different experiments.

A similar method also based on the combination of a set of cross-power spectra has been first used to obtain recent results from the first year WMAP data (Hinshaw et al. 2003). The main difference between the method presented is this paper and the WMAP one is the determination of the cross-correlation matrix (see Sect.3) of the corrected cross-power spectra used both for the combination of these into a single power spectra and for the estimation of the error bars on the latter. The WMAP team estimates the cross-correlation matrix from a model of the data. This includes specific terms related to the WMAP data such as the contribution from point sources and the uncertainties on the beam window functions as well as a term related to the CMB anisotropies which is estimated from a fiducial model. The WMAP cross-correlation matrix, used for the combination of the cross-power spectra, does not incorporate the effects of mode coupling. In a further step, they account for the mode coupling and the dependence on the fiducial CMB model for the computation of the uncertainties on the final power spectrum.

By contrast, the method presented here computes the cross-correlation matrix directly from the cross-power spectra estimated from the data. This allows us to include naturally the mode coupling in this matrix. Further, this permits the computation of analytical error bars (as described in Sect. 3) which are very compatible with those obtained from simulations (see Sect. 5). Because of the above, this method can be applied without modification to the estimation of the power spectrum of the correlated signal between a set of maps of the sky coming from multiple instruments with potentially different sky coverages. For example, we have used this method on ARCHEOPS data for the estimation of the CMB angular power spectrum and the contribution from foregrounds to this one (Tristram et al. 2005). We have also used it for the estimation of the foreground emission at the sub-millimeter and millimeter wavelength by cross-correlating the ARCHEOPS data with foreground dust templates.

In Sect. 2, we remind to the reader the computation of the cross-power spectra from 'pseudo' cross-power spectra. In Sect. 3, we specify the correlation between cross-power spectra and between multipoles. Analytical expressions for the error bars and the covariance matrix for each cross-power spectra are derived. Section 4 discusses the combination of the cross-spectra from either a single full data set (Sect. 4.1) or several independent experiments (Sect. 4.2). Finally, Xspect is applied to simulations of the ARCHEOPS balloon-borne experiment in Sect. 5.

2 CROSS-POWER SPECTRA

Under the assumption of uncorrelated noise between detectors, the cross-power spectrum computed from sky maps is a non noise-biased estimate of the angular power spectrum. In general, when computing the C_ℓs, other instrumental effects as beam smoothing, incomplete sky coverage and time ordered data filtering need to be taken into account. These effects and the way to correct them have been deeply covered in the literature for classical 'pseudo-C_ℓ' estimators (Szapudi et al. 2001; Hivon et al. 2002; Hansen et al. 2002) which are noise biased as they use directly the auto power spectrum of each detector map. As shown in the following, these corrections can be extended to the case of cross-power spectra.

The CMB temperature anisotropies, ΔT, over the full-sky can be decomposed into spherical harmonics as follows,

$$\Delta T(\vec{n}) = \sum_{\ell m} a_{\ell m} Y_{\ell m}(\vec{n}) \tag{1}$$

where the coefficient $a_{\ell m}$ are given by

$$a_{\ell m} = \int \Delta T(\hat{n}) Y_{\ell m}(\hat{n}) d\Omega \ . \tag{2}$$

The CMB temperature field ΔT predicted by most inflationary models (Liddle & Lyth 2000; Linde et al. 1999; Hu et al. 1997) is in general Gaussian distributed so that the ensemble average of the $a_{\ell m}$ coefficients are

$$\langle a_{\ell m} \rangle = 0 \quad (3)$$

$$\langle a_{\ell m} a^*_{\ell' m'} \rangle = \langle C_\ell \rangle \delta_{\ell \ell'} \delta_{m m'} \quad (4)$$

An unbiased estimate of the CMB temperature power spectrum $\langle C_\ell \rangle$ is therefore given by

$$\widehat{C_\ell} = \sum_{m=-\ell}^{\ell} \frac{|a_{\ell m}|^2}{2\ell+1} \ . \quad (5)$$

Ground-based and balloon-borne CMB experiments present an inhomogeneous sky coverage. On the other hand, satellite experiments like COBE, WMAP and Planck, although they provide full-sky maps, residuals of foreground contamination in the Galactic plane and point sources contamination make impossible to use the complete maps when computing the CMB angular power spectrum. Furthermore, for most CMB experiments, the noise properties vary considerably due to different redundancies between pixels of the same map. So obtaining an estimate of the power spectrum requires a differential weighting of pixels within the same map which translates into an effective inhomogeneous sky coverage.

The decomposition in spherical harmonics of the observed temperature anisotropies including weighting can be written for a single detector as follows

$$d_{\ell m} = \int d\Omega \, T^{\rm map}(\hat{n}) W(\hat{n}) Y_{\ell m}(\hat{n}) \quad (6)$$

$$\simeq \sum_{p=1}^{N_{\rm pix}} \Omega_p \, T_p^{\rm map} \, W(\hat{n}_p) \, Y_{\ell m}(\hat{n}_p), \quad (7)$$

where $\Omega_p = \frac{4\pi}{N_{\rm pix}}$ for equal pixels (as in HEALPix pixelization, Gorski et al. 1998) and W is the mask applied to the input sky temperature T^{map}. This temperature can be decomposed into signal and noise, $T^{map} = T^{signal} + T^{noise}$ which are assumed to be uncorrelated, *i.e.*

$$\left\langle T^{signal} \, T^{noise} \right\rangle = 0 \ . \quad (8)$$

The effect of a non-homogeneous coverage of the sky can be described in spherical harmonics (Peebles 1973) by a mode-mode coupling matrix $M_{\ell\ell'}$ which depends only on the angular power spectrum of the weighting scheme (hereafter weighting mask) applied to the sky to account for the incomplete coverage, the removal of the Galactic plane and the inhomogeneous noise properties of the detector.

Thus, the 'pseudo-C_ℓ' estimator D_ℓ is defined as follows

$$\widehat{D_\ell} = \frac{1}{2\ell+1} \sum_{m=-\ell}^{\ell} |d_{\ell m}|^2 \ . \quad (9)$$

The relation that links the 'pseudo' power spectrum, directly measured on the sky, and the power spectrum C_ℓ of the CMB anisotropies is given by

$$\widehat{D_\ell} = \sum_{\ell'} M_{\ell\ell'} |p_{\ell'} B_{\ell'}|^2 F_{\ell'} \langle C_{\ell'} \rangle + \langle N_\ell \rangle \quad (10)$$

where B_ℓ is the beam transfer function describing the beam smoothing effect; p_ℓ is the transfer function of the pixelization scheme of the map describing the effect of smoothing due to the finite pixel size and geometry; F_ℓ is an effective function that represents any filtering applied to the time ordered data; and $\langle N_\ell \rangle$ is the noise power spectrum.

2.1 Pseudo cross-power spectrum

An unbiased estimate of the cross-power spectrum C_ℓ^{AB} between the full sky maps of two independent and perfect detectors A and B can be obtained from

$$\widehat{C_\ell^{AB}} = \frac{1}{2\ell+1} \sum_{m=-\ell}^{\ell} a^A_{\ell m} \, a^{B\,*}_{\ell m} . \quad (11)$$

where $a^A_{\ell m}$ and $a^B_{\ell m}$ are the coefficients of the spherical harmonic decomposition of maps A and B respectively.

In the same way, we can compute the 'pseudo' cross-power spectrum $\widehat{D_\ell^{AB}}$ between any two detectors A and B by generalizing Eq. 10

$$\widehat{D_\ell^{AB}} = \sum_{\ell'} M^{AB}_{\ell\ell'} |p_{\ell'}|^2 B^A_{\ell'} B^B_{\ell'} F^{AB}_{\ell'} \left\langle C^{AB}_{\ell'} \right\rangle + \left\langle N^{AB}_\ell \right\rangle \ . \quad (12)$$

Each of the terms in Eq. 12 is described in more details in the following subsections.

2.2 Noise cross-power spectrum, N_ℓ^{AB}

The main advantage of using cross-power spectra is that the noise is generally uncorrelated between different detectors

$$\left\langle n^A_{\ell m} n^{B\,*}_{\ell' m'} \right\rangle = 0 \ . \quad (13)$$

This assumption will be maintained throughout this paper.

Thus, the cross-power spectra are straightforward estimates of the angular power spectrum on the sky and for two different detectors (*i.e.* $A \neq B$), the 'pseudo' cross-power spectrum reads

$$\widehat{D_\ell^{AB}} = \sum_{\ell'} M^{AB}_{\ell\ell'} |p_{\ell'}|^2 B^A_{\ell'} B^B_{\ell'} F^{AB}_{\ell'} \left\langle C^{AB}_{\ell'} \right\rangle \ . \quad (14)$$

2.3 Coupling kernel matrix, $M_{\ell\ell'}^{AB}$

The coupling kernel matrix $M_{\ell\ell'}$, introduced in Eq. 10 and described in details in Hivon et al. 2002, reads

$$M_{\ell\ell'} = \frac{2\ell'+1}{4\pi} \sum_{\ell''} (2\ell''+1) \mathcal{W}_{\ell''} \begin{pmatrix} \ell & \ell' & \ell'' \\ 0 & 0 & 0 \end{pmatrix}^2 \quad (15)$$

where $\mathcal{W}_\ell = \frac{1}{2\ell+1} \sum_{m=-\ell}^{\ell} |w_{\ell m}|^2$ is the power spectrum of the mask. It takes into account the mask applied to the data where mask represents both the sky coverage and the weighting scheme.

Equation 15 can be easily generalized to the case of two different masks applied respectively to each map of the two detectors involved in the cross-power spectrum calculation. Replacing the quadratic terms $|w_{\ell m}|^2$ by $\left\langle w^A_{\ell m} w^{B*}_{\ell m} \right\rangle$ in the computation of Eq. 15 leads to

$$M^{AB}_{\ell\ell'} = \frac{2\ell'+1}{4\pi} \sum_{\ell''} (2\ell''+1) \mathcal{W}^{AB}_{\ell''} \begin{pmatrix} \ell & \ell' & \ell'' \\ 0 & 0 & 0 \end{pmatrix}^2 \quad (16)$$

where $\mathcal{W}_\ell^{AB} = \frac{1}{2\ell+1}\sum_{m=-\ell}^{\ell} w_{\ell m}^A w_{\ell m}^{B*}$, the cross-power spectrum of the masks.

This property allows us to deal with independent masks representing different sky coverages and to apply an appropriate specific weighting scheme to each detector map. Note that the correction in the multipole space discussed here is fully equivalent to an appropriate normalization of the cross correlation between the two sky masked maps in real space. This analogy is important as it helps to understand why no fully overlapping masks for the input maps can be considered.

2.4 Filter function, F_ℓ^{AB}

The filter function F_ℓ accounts for the filtering of the time ordered data which is generally needed in most CMB experiments either to avoid systematic effects or to reduce correlated low frequency noise. The time domain filtering is performed along a preferred direction on the sky (scanning direction) and so leads commonly to an anisotropic sky even if the assumption of initial isotropic temperature fluctuations holds. In this case, the estimates of the angular power spectrum provided by Eq. 10 and Eq. 14 are not exact any more and should be corrected for a function both in ℓ and m, $F_{\ell,m}$. Obtaining accurate estimates of such a correction is particularly complex and for most cases, as proposed by Hivon et al. 2002, the correction for an effective F_ℓ is good enough for the accuracy required in the reconstruction of the CMB power spectrum. The F_ℓ function can be, for example, computed via Monte-Carlo simulations of the sky from which mock time ordered data are produced for each of the detectors involved and then filtered.

From an initial theoretical CMB power spectrum, we compute a large number of realizations of the sky using the HEALPix software *synfast* (Gorski et al. 1998) and compute mock time ordered data from the scanning strategy of each detector. Maps are then computed with and without filtering before re-projection. The F_ℓ function is obtained from the mean ratio of the 'pseudo' power spectra of the filtered and not filtered maps. The latter are obtained using the HEALPix software *anafast*.

In the case of the cross-power spectra and considering the previous approximation, an effective filter function $F_\ell^{AB} = \sqrt{F_\ell^A F_\ell^B}$ will be considered in the following. As defined, the effective filtering function allows us to consider detectors for which the time domain filtering is different.

Note that, for nearly white noise and all-sky surveys such as WMAP or Planck missions, filtering may not be required and thus $F_\ell = 1$.

2.5 Beam window function, B_ℓ^A

The beam window function B_ℓ describes the smoothing effect of the main instrumental beam under the hypothesis of circularity. The latter does not hold in general as for most experiments the main beam pattern is asymmetric. As beam uncertainties have become the most important source of systematic errors, taking into account the asymmetry of the beam pattern is necessary. Several solutions have been proposed either circularizing the beam (Wu et al. 2000; Page et al. 2003) or assuming an elliptical Gaussian beam (Souradeep & Ratra 2001; Fosalba et al. 2002). The work of Wandelt & Gorski 2001 presents how to convolve *exactly* two band limited but otherwise arbitrary functions on the sphere - which can be the 4-π beam pattern and the sky descriptions. An analytic framework for studying the leading order effects of a non-circular beam on the CMB power spectrum estimation is proposed in Mitra et al. 2004.

The authors of this paper present *Asymfast* (Tristram et al. 2004), a general method to estimate an effective B_ℓ function taking into account the asymmetry of the main beam and the scanning strategy. *Asymfast* is based on a decomposition of the main beam pattern into a linear combination of Gaussians which permits fast convolution in the spherical harmonic space along the scanning strategy.

2.6 Cross-power spectrum from 'pseudo' cross-power spectrum

The cross-power spectrum C_ℓ^{AB} can be obtained from the 'pseudo' cross-power spectrum D_ℓ^{AB} by resolving Eq. 12 which leads to invert the coupling kernel matrix ${M_{\ell\ell'}}^{AB}$. In general for complex sky coverage and weighting schemes, this matrix is singular and can not be inverted directly. To avoid this problem, Hivon et al. 2002 proposed the binning of the coupling kernel matrix which reduces considerably the complex correlation pattern in the C_ℓs introduced by the applied mask. The binning is obtained by applying the operators $P_{b\ell}$ and $Q_{\ell b}$ as follows

$$\widehat{C_b^{AB}} = P_{b\ell}\widehat{C_\ell^{AB}} \quad (17)$$

$$\widehat{D_b^{AB}} = P_{b\ell}\widehat{D_\ell^{AB}} \quad (18)$$

$$Q_{\ell b} = P_{b\ell}^{-1}. \quad (19)$$

The solution of Eq. 14 in the new base reads

$$\widehat{C_b^{AB}} = \mathcal{M}_{bb'}^{-1}\widehat{D_{b'}^{AB}} \quad (20)$$

with

$$\mathcal{M}_{bb'} = P_{b\ell}\left(M_{\ell\ell'}^{AB} F_{\ell'} p_{\ell'}^2 B_{\ell'}^A B_{\ell'}^B\right) Q_{\ell' b'}. \quad (21)$$

As the correlation between multipoles ℓ depends very much on the instrumental setup, the sky coverage and the weighting scheme, the binning has to be defined for each experiment. It is a compromise between a good multipole sampling and low correlations between adjacent bins.

Hereafter to avoid confusion and makes the notation simpler all equations will be written in ℓ instead of b.

3 CROSS-CORRELATION MATRIX - ANALYTICAL ERROR BARS AND COVARIANCE MATRIX

From N input maps we can obtain $N(N-1)/2$ cross-power spectra C_ℓ^{AB} $(A \neq B)$ which are unbiased estimates of the angular power spectrum but which are obviously not independent. In this section, we describe the estimation of the cross-correlation matrix between cross-spectra and between multipoles. We show how the error bars and the covariance matrix in multipole space can be deduced for each cross-power spectra.

3.1 The cross-correlation matrix, Ξ

Given a sky map from a detector A, it can be combined to each of the other detector maps to form $N-1$ cross-power spectra which will therefore be highly correlated. Furthermore, due to the masking we also expect that each cross-power spectra will be correlated for adjacent multipoles and thus, correlations between adjacent multipoles will be also present between different cross-power spectra. To describe this complexity we define the cross-correlation matrix

$$\Xi^{AB,CD}_{\ell\ell'} = \left\langle \left(C^{AB}_\ell - \left\langle C^{AB}_\ell \right\rangle\right) \left(C^{CD}_{\ell'} - \left\langle C^{CD}_{\ell'} \right\rangle\right)^* \right\rangle$$

of the cross-power spectra AB ($A \neq B$) and CD ($C \neq D$) which can be fully computed as shown in the following.

From Eq. 14 we can express the 'pseudo' cross-power spectrum between detectors A and B as follows

$$\widehat{D^{AB}_\ell} \;=\; \mathcal{M}^{AB}_{\ell\ell'} \widehat{C^{AB}_{\ell'}} \tag{22}$$

where $\mathcal{M}^{AB}_{\ell\ell'} = M^{AB}_{\ell\ell'} E^A_{\ell'} E^B_{\ell'}$ and $E_\ell = p_\ell B_\ell \sqrt{F_\ell}$ and therefore the corrected cross-power spectrum for detectors A and B is given by

$$\widehat{C^{AB}_\ell} = \left(\mathcal{M}^{AB}_{\ell\ell'}\right)^{-1} \widehat{D^{AB}_{\ell'}}. \tag{23}$$

Using the above expression and following the previous definition, the cross-correlation matrix $\Xi^{AB,CD}_{\ell\ell'}$ reads

$$\begin{aligned}
\Xi^{AB,CD}_{\ell\ell'} &\equiv \left\langle \Delta C^{AB}_\ell \Delta C^{CD\,*}_{\ell'} \right\rangle \\
&= \left\langle \mathcal{M}^{AB\,-1}_{\ell\ell_1} \Delta D^{AB}_{\ell_1} \left(\mathcal{M}^{CD\,-1}_{\ell'\ell_2} \Delta D^{CD}_{\ell_2}\right)^* \right\rangle \\
&= \mathcal{M}^{AB\,-1}_{\ell\ell_1} \left\langle \Delta D^{AB}_{\ell_1} \Delta D^{CD\,*}_{\ell_2} \right\rangle (\mathcal{M}^{CD\,-1}_{\ell'\ell_2})^T
\end{aligned} \tag{24}$$

The above equation as it stands can not be used in practice for ℓ above ~ 10 as the calculation of

$$\begin{aligned}
\left\langle \Delta D^{AB}_{\ell_1} \Delta D^{CD\,*}_{\ell_2} \right\rangle = \frac{1}{(2\ell+1)(2\ell'+1)} \sum_{mm'} \sum_{\ell_1 m_1} \sum_{\ell_2 m_2} \\
C^{AC}_{\ell_1} C^{BD}_{\ell_2} K^A_{\ell m \ell_1 m_1} K^C_{\ell' m' \ell_1 m_1} K^B_{\ell m \ell_2 m_2} K^D_{\ell' m' \ell_2 m_2}
\end{aligned} \tag{25}$$

described in Appendix A, is numerically unstable (Varshalovich et al. 1988). However, for high multipoles and sufficiently large sky coverage (as it is the case for satellite missions as WMAP and Planck) it can be simplified (Efstathiou 2004) by replacing $C^{AC}_{\ell_1}$ and $C^{BD}_{\ell_2}$ by $C^{AC}_{\ell'}$ and $C^{BD}_{\ell'}$ respectively and then applying the completeness relation for spherical harmonics (Varshalovich et al. 1988). This is because the $K_{\ell m \ell' m'}$, which is diagonal for full sky coverage, is quasi-diagonal for large sky coverage.

Under the above hypothesis and following Appendix A, the cross-correlation matrix reads

$$\begin{aligned}
\Xi^{AB,CD}_{\ell\ell'} \;=\; \mathcal{M}^{AB\,-1}_{\ell\ell_1} \left[\frac{\mathcal{M}^{(2)}_{\ell_1\ell_2}\left(W^{AC,BD}\right) C^{AC}_{\ell_1} C^{BD}_{\ell_2}}{2\ell_2+1} + \right. \\
\left. \frac{\mathcal{M}^{(2)}_{\ell_1\ell_2}\left(W^{AD,BC}\right) C^{AD}_{\ell_1} C^{BC}_{\ell_2}}{2\ell_2+1} \right] (\mathcal{M}^{CD\,-1}_{\ell'\ell_2})^T
\end{aligned} \tag{26}$$

where

$$\mathcal{M}^{(2)}_{l1l2}\left(W^{AC,BD}\right) = E^A_{l1} E^C_{l1} M^{(2)}_{l1l2}\left(W^{AC,BD}\right) E^B_{l2} E^D_{l2}$$

and $M^{(2)}$ is the quadratic coupling kernel matrix

$$\begin{aligned}
&M^{(2)}_{\ell_1\ell_2}\left(W^{AB,CD}\right) = \\
&\frac{(2l2+1)}{4\pi} \sum_{l3} (2l3+1) W^{AB,CD}_{\ell_3} \begin{pmatrix} l1 & l2 & l3 \\ 0 & 0 & 0 \end{pmatrix}^2
\end{aligned} \tag{27}$$

associated to the cross-power spectrum of the product of the masks $W^{AB,CD} = \frac{1}{2\ell+1} \sum_m w^{(2)\,AB}_{\ell m} w^{(2)\,CD*}_{\ell m}$. The $w^{(2)\,AB}_{\ell m}$ represents the spherical harmonic coefficients for the product of the masks associated to detectors A and B.

Equation 26 can be further simplified by assuming uniform weighting and the same sky coverage for all detectors, as well as a diagonal dominated coupling kernel matrix,

$$\Xi^{AB,CD}_{\ell\ell'} \simeq \frac{1}{\nu_{\ell'}} \left[C^{AC}_\ell C^{BD}_{\ell'} + C^{AD}_\ell C^{BC}_{\ell'} \right] \tag{28}$$

In this case, the effect of a non-homogeneous sky coverage is represented by a simple function ν_ℓ which can be associated to the effective number of degrees of freedom in the $\chi^2_{\nu_\ell}$ distribution of the C_ℓs over the sky (see Hivon et al. 2002)

$$\nu_\ell = (2\ell+1) \Delta_\ell \frac{w_2^2}{w_4} \tag{29}$$

where w_i is the i-th moment of the mask

$$w_i = \frac{1}{4\pi} \int_{4\pi} d\Omega W^i(\Omega)\,. \tag{30}$$

In Eq. 26 and 28, the C_ℓ can be either cross-power spectra or auto-power spectra depending on the combination of A, B, C and D (the only condition is $A \neq B$ and $C \neq D$). In one hand, noise terms, as included in the auto-power spectra, appear in the analytical form of the correlation matrix Ξ. On the other hand, for a set of 4 independant detectors ($A \neq B \neq C \neq D$), the correlation matrix is the variance of the signal.

3.2 Covariance Matrix and error bars associated to the cross-power spectra

It is important to notice that the cross-correlation matrix contains all the needed information to perform error bars and covariance matrix for each single cross-power spectrum. From Eq. 26 (or Eq. 28 for the approximated form), the covariance matrix providing the correlation between adjacent multipoles is given by

$$\begin{aligned}
Cov^{AB}(\ell,\ell') &= \Xi^{AB,AB}_{\ell\ell'} \\
&\simeq \frac{1}{\nu_{\ell'}} \left[C^{AB}_\ell C^{AB}_{\ell'} + C^{AA}_\ell C^{BB}_{\ell'} \right]
\end{aligned} \tag{31}$$

In the same way, we can also write the variance of each cross-power spectra which corresponds to the error bars $\Delta {C_\ell}^{AB}$ associated to each cross-power spectra

$$\begin{aligned}
\left(\Delta {C_\ell}^{AB}\right)^2 &= \Xi^{AB,AB}_{\ell\ell} \\
&\simeq \frac{1}{\nu_\ell} \left[\left(C^{AB}_\ell\right)^2 + C^{AA}_\ell C^{BB}_\ell \right]
\end{aligned} \tag{32}$$

In these cases, instrumental noise appears in the auto-power spectra C^{XX}_ℓ (for which $N^{XX}_\ell \neq 0$). As it is computed directly from the data, no estimation of the noise is needed.

4 COMBINED ANGULAR POWER SPECTRUM

This section describes the estimation of the final CMB angular power spectrum and the error bars associated to it using the corrected cross-power spectra described in Sect. 2 in addition to the cross-correlation matrix computed in Sect. 3. We propose a simple but efficient way to combine them by maximizing a quadratic likelihood function and to deduce the final error bars from the cross-correlation matrix. For this paper we have considered a very general form for the likelihood function limited to a simple CMB plus noise model. However, the likelihood function can be adapted more specifically to the data, for example to include point sources as it is the case for the WMAP results presented in Hinshaw et al. 2003. More generally, it could be extended to algorithms of spectral matching decomposition (*e.g.* Delabrouille et al. 2003). In the following, we present how this method can be used to provide both an estimate of the C_ℓs from a full data set (Sect. 4.1) and of the angular power spectrum of common sky fluctuations between maps coming from two or more independent surveys (Sect. 4.2).

4.1 Gaussian approximated linear combination of the cross-power spectra

Once all possible cross-power spectra have been computed from a data set, we dispose of $N(N-1)/2$ different but not independent measurements of the angular power spectrum, C_ℓs. To combine them and obtain the best estimate of the power spectrum $\widetilde{C_\ell}$, we maximize the Gaussian approximated likelihood function

$$-2\ln\mathcal{L} = \sum_{ij}\left[(C_\ell^i - \widetilde{C_\ell})|\Xi^{-1}|^{ij}_{\ell\ell'}(C_{\ell'}^j - \widetilde{C_{\ell'}})\right] \tag{33}$$

where $|\Xi_{\ell\ell'}|^{ij} = \Xi^{AB,CD}_{\ell\ell'}$ is the cross-correlation matrix of the cross-power spectra described before (i and $j \in \{AB, A\neq B\}$). The auto-power spectra are not considered.

From this and neglecting the correlation between adjacent multipoles, it is straightforward to show that the estimate of the angular power spectrum is

$$\widetilde{C_\ell} = \frac{1}{2}\frac{\sum_{ij}\left[|\Xi^{-1}|^{ij}_{\ell\ell}C_\ell^j + C_\ell^i|\Xi^{-1}|^{ij}_{\ell\ell}\right]}{\sum_{ij}|\Xi^{-1}|^{ij}_{\ell\ell}} \tag{34}$$

The final covariance matrix can be obtained from Eq. 33,

$$Cov(\ell,\ell') = \frac{1}{\sum_{ij}|\Xi^{-1}|^{ij}_{\ell\ell'}} \tag{35}$$

and the final error bars are given by

$$\left(\Delta\widetilde{C_\ell}\right)^2 = \frac{1}{\sum_{ij}|\Xi^{-1}|^{ij}_{\ell\ell}}\,. \tag{36}$$

Depending on the cross-correlation between cross-power spectra, the instrumental noise variance is reduced by a factor comprised between N, the number of independant detectors, and $N(N-1)/2$, the number of cross-power spectra.

For the noise dominated case, the correlation between different cross-power spectra can be neglected and the cross-correlation matrix Ξ becomes diagonal (see eq. 26 and 28). The values in the diagonal are the $N(N-1)/2$ products of 2 auto-power spectra (including noise). The variance of final power spectrum is then proportional to $\frac{1}{N(N-1)/2}$. In any case, when combining cross-power spectra, the upper limit for the variance comes from the combination of N independent detectors (proportional to $\frac{1}{N}$).

4.2 Common angular power spectrum

The Xspect formalism allows us to compare two or more different sets of sky maps coming from two or more independent experiments. In this respect, the quantity of interest is the power spectrum of the common fluctuations on the sky with the same physical origin. We will call the latter common angular power spectrum C_ℓ^{common} for simplicity. In fact, if we compare for example two sets of CMB maps at low and high frequencies, the foreground contamination will be different and we can expect to obtain a better estimation of the CMB power spectrum. In the same way, for two different experiments, systematic effects will be decorrelated and will not contribute to the common angular power spectrum calculated from them. In addition, template maps of foreground emission can be correlated to the CMB experiments maps to monitor and to subtract foreground residuals.

To simplify the notation we will only consider two sets of sky maps A and B, corresponding to N_A and N_B detectors respectively. Following the previous paragraph considerations, by cross-correlating each detector map from A which each detector map from B and correcting the 'pseudo' cross-power spectra as described before, we can form $N_A \times N_B$ cross-power spectra which are unbiased estimates of the common power spectrum but not fully independent.

The cross-power spectra formed in this way can be noted $C_\ell^{A_i,B_j}$ and their cross-correlation matrix $\Xi^{A_iB_j,A_uB_v}_{\ell\ell'}$ reads

$$\Xi^{A_iB_j,A_uB_v}_{\ell\ell'} = \mathcal{M}^{A_iB_j\,-1}_{\ell\ell_1}\left\langle \Delta D^{A_iB_j}_{\ell_1}\Delta D^{A_uB_v\,*}_{\ell_2}\right\rangle(\mathcal{M}^{A_uB_v\,-1}_{\ell'\ell_2})^T \tag{37}$$

which can be computed using previous approximations.

Finally, equations 34 and 36 are used to obtain the estimate of the common angular power spectrum $\widetilde{C_\ell}^{common}$ and the error bars associated to it.

This method allows us to deal naturally with very different experimental configurations such as for example completely different scanning strategies, different timeline filtering and different beam patterns for each of the detectors involved. Furthermore, it can be easily generalized to work with non CMB data such as maps of the Sunyaev-Zel'dovich effect in clusters of Galaxies or maps of mass fluctuations from weak lensing observations.

5 XSPECT APPLIED TO ARCHEOPS BALLOON-BORNE EXPERIMENT

Xspect was mainly developed to measure the CMB temperature angular power spectrum from the Archeops data as well as to compare these data to other observations of the sky as for example those from the WMAP satellite.

ARCHEOPS (Benoît et al. 2003) is a balloon-borne experiment conceived as a precursor of the PLANCK High Frequency Instrument[1]. It consists of a 1.5 m off-axis Gregorian telescope and of an array of 21 photometers cooled down to $\sim$ 100 mK and which operates in 4 frequency bands: 143 and 217 GHz (CMB channels) and 353 and 545 GHz (Galactic channels). For the latest flight campaign, the entire ARCHEOPS data cover about $\sim$ 30% of the sky, including the Galactic plane.

5.1 Simulations of the Archeops data set

As a first step in the application of Xspect to the ARCHEOPS data set, we have produced 500 simulations of the sky observed by ARCHEOPS including both the CMB signal and the detector noise for the six most sensitive ARCHEOPS detectors at 143 and 217 GHz.

These simulations are computed from realizations of the CMB sky at $nside = 512$ (corresponding to a pixel size of $\sim$ 7 arcmin) for the ARCHEOPS best-fit CMB model presented in Benoît et al. 2003. The sky maps are convolved by the main beam pattern of each of the $N_{detec} = 6$ ARCHEOPS detectors using the beam transfer function and then deprojected following the ARCHEOPS scanning strategy to produce mock ARCHEOPS timelines. The beam transfer functions were computed individually for each detector from Jupiter's crossings in the data using the *Asymfast* method presented in Tristram et al. 2004.

The detector noise is computed from the time power spectrum of each of the detectors and added to the mock signal timelines. The method used for the estimation of the time noise power spectra is described in details in Amblard & Hamilton 2004. To suppress $1/f$-noise, remaining atmospheric and galactic contamination as well as non-stationary high frequency noise, the ARCHEOPS time streams are Fourier filtered using a bandpass filter between 0.1 and 38 Hz. We apply the same filtering to the simulated timelines before projection. The corresponding multipole filtering function F_ℓ was independently calculated by specific simulations. The filtered timelines are then reprojected using the ARCHEOPS scanning strategy to produce N_{detec} simulated co-added maps for each simulation run.

A Galactic mask deduced from a SFD IRAS map (Schlegel et al. 1998), extrapolated to 353 GHz, using a cut in amplitude (greater than 0.5 MJy.str) is applied to the simulated maps. This reduces the total ARCHEOPS coverage to $\sim$ 20% of the sky. We have used two different weighting schemes on the maps. The first one is an uniform weighting and the second one, a $1/\sigma^2_{pix}$ weighting per pixel and per detector, where σ^2_{pix} is the noise variance for the given pixel.

Then we apply the Xspect method to each simulations-run. The $N_{detec}(N_{detec}-1)/2$ cross-power spectra are computed with their associated cross-correlation matrices and combined as described in Sect. 4.1 using the Gaussian approximation of the likelihood function.

In addition to the above simulations, we produced, in the same way, 500 non noisy simulations from which we can extract for example the sample variance for the ARCHEOPS coverage.

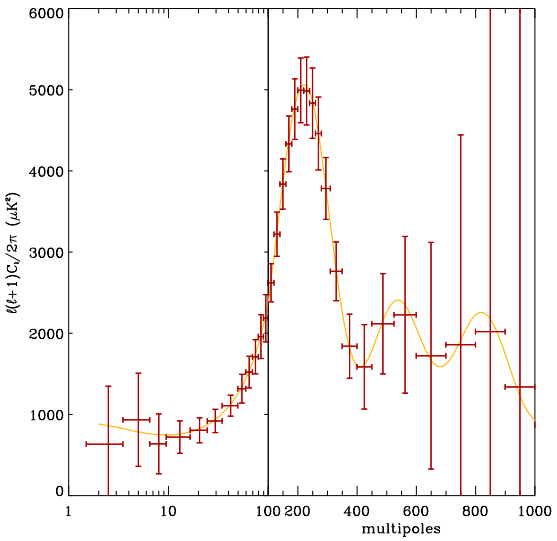

Figure 1. Mean angular power spectrum obtained from 500 simulations of ARCHEOPS observations of the CMB sky (see text for details). We use the ARCHEOPS best-fit model (Benoît et al. 2003) to produce CMB maps which are smeared out using the beam pattern of each of the six most sensitive ARCHEOPS detectors and deprojected into mock ARCHEOPS timelines. Noise is then added up for each detector and the resulting timelines projected into sky maps are analyzed using Xspect. The error bars shown here are computed analytically as described in previous sections. The Xspect estimate of the angular power spectrum (in red) is an unbiased estimate of the input CMB model (in yellow).

Figure 1 shows the mean angular power spectrum computed from the angular power spectrum estimates obtained for each of the 500-simulations runs. The error bars are analytically computed. We observe that the Gaussian approximated combination of cross-power spectra is an unbiased estimate of the input CMB model for the angular power spectrum. This mean angular power spectrum is a combination of two weighting schemes. Up to $\ell = 90$, we use uniform weighting whereas, for larger ℓ, a mask inversely proportional to the noise in each of the pixels has been applied. This allows us to choose the smaller error bars in each region.

Figure 2 shows analytic estimates of the error bars in the final angular power spectrum compared to the dispersion for each multipole bin over the 500 Monte-Carlo simulations. The ARCHEOPS sky coverage is very inhomogeneous due to the particular choice of the scanning strategy which tries to maximize the area of the sky observed ($\sim$ 30%) in a very reduced amount of observation time (less than 12 hours). ARCHEOPS performs large circles on the sky that leads to a quasi ring-like coverage with a large uncovered region at the center of the ring as shown on Fig. 3. This implies that the approximation used to obtain Eq. 28 is not valid, especially at low multipoles, and therefore the error bars obtained analytically (red solid line) are underestimated up to $\sim$ 20% at very low ℓ with a mean of $\sim$ 10%. By computing $\Xi^{AB,CD}_{\ell\ell'}$ as given by Eq. 26, the analytic error bars (yellow solid line) increase as expected and fit much better the dispersion in

[1] http://www.planck-hfi.org

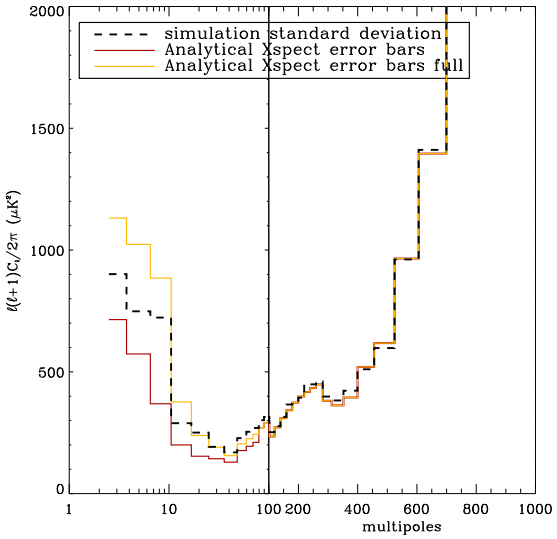

Figure 2. Error bars for the ARCHEOPS data computed analytically, from Eq. 28 (red solid line) and from Eq. 26 (yellow solid line). They are compared to the standard deviation of $N_{simu} = 500$ simulations (black dashed line). Differences essentially originate from the extremely inhomogeneous ARCHEOPS sky coverage (see text for details).

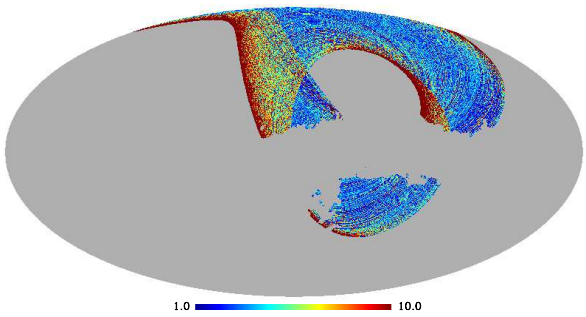

Figure 3. Sky coverage and weighting scheme applied to the sky map ($nside = 512$) obtained from the ARCHEOPS most sensitive detector at 143 GHz. We observe a ring-like structure with a large uncovered area in the center and highly redundant areas on the edges of the ring.

the simulations (black dashed line). The agreement is then within 10% over the full range of multipoles with a mean of 1.5%. Equivalent results are obtained using non noisy simulations.

5.2 Application to the ARCHEOPS data

Xspect has been applied to the data from the last ARCHEOPS flight campaign using the six most sensitive bolometers as in the simulations presented above. The results of this analysis is presented in a collaboration paper (Tristram et al. 2005). Cross-correlation with WMAP maps is also under study in order to assess the electromagnetic spectrum of the CMB anisotropies from 40 to 217 GHz.

6 SUMMARY AND CONCLUSIONS

In this paper, we have presented a method, Xspect, for the obtention of the CMB angular power spectrum with analytical error bars based on four main steps:

(i) Given N independent input sky maps from different detectors either from a single experiment or from multiple ones, we estimate $N(N-1)/2$ 'pseudo' cross-power spectra as well as N 'pseudo' auto-power spectra using the HEALPix package (Gorski et al. 1998).

(ii) Cross-power spectra are obtained by correcting the 'pseudo' power spectra for weighting scheme, beam smoothing and filtering as discussed in Section 2. In the same way, we compute auto-power spectra with noise. Xspect can deal with different and complex weighting schemes for each of the detectors involved. The coupling matrix, beam and filtering transfer functions are precomputed for each pair of detectors.

(iii) We compute the full cross-correlation matrix, $\Xi_{\ell\ell'}^{AB,CD}$, between cross-power spectra AB ($A \neq B$) and CD ($C \neq D$) (Section 3.1) from which we can extract the covariance matrix and the error bars for each cross-power spectra (Sect 3.2).

(iv) Finally, the corrected cross-power spectra are combined into a single angular power spectrum using their cross-correlation matrices which are assumed to be diagonal in multipole space. The Gaussian approximation of the likelihood function is fully justified in the large multipole range. In addition, analytical estimates for the error bars and for the covariance matrix are computed (Section 4). The covariance matrix can be used to check the degree of correlation between multipoles.

As this method estimates the angular power spectrum using 'pseudo' cross-power spectra, we can obtain a non noise-biased power spectrum avoiding the estimation of the noise power spectra which requires heavy Monte-Carlo simulations. Equally, this permits the estimation of analytical error bars which are compatible to those computed from simulations. Furthermore, Xspect allows us to obtain the angular power spectrum of common sky fluctuations between two or more experiments. Associated to other surveys used as templates, it can provide estimations of systematic residuals or astrophysical contaminations. Nevertheless, Xspect computes only the common structures between maps, assuming a single physical component. This means that, for CMB purposes, foregrounds and systematics must be subtracted beforehand.

Xspect has been successfully applied to simulations of the ARCHEOPS experiment which presents an inhomogeneous sky coverage and detectors with unequal sensitivities. Even for a balloon-borne experiment that can be compared to satellite missions neither in noise level nor in sky coverage, the analytical estimates of the errors computed with Xspect are accurate within few percents. This property is of great interest when producing Monte Carlo simulations in the process of testing and improving the estimation of the C_ℓs or when checking the robustness of the data analysis with respect to the various choices of mask, filtering or binning. The application of Xspect to the ARCHEOPS data set will be published by the ARCHEOPS collaboration shortly (Tristram et al. 2005).

For the WMAP satellite, which covers the full sky in a very homogeneous way, it was also interesting to check the analytical estimates of the error bars. Xspect analytical errors are equivalent to those provided by the WMAP team within 15% with a mean of 1.8%. This agreement is satisfactory as our analysis was more basic than the one used to derive the first year WMAP results presented in Hinshaw et al. 2003. In particular all maps at all multipoles were used without any point-source specific treatment and only two weighting schemes were applied.

The extension of Xspect to CMB polarization maps is under development. As for the temperature power spectrum, the C_ℓ^{EE} and C_ℓ^{BB} power spectra obtained directly from a single set of I, Q and U maps via a 'pseudo' power spectrum estimator are noise biased. A 'pseudo' cross-power spectrum estimator adapted to polarization can solve this problem by using independent sets of I, Q and U maps.

ACKNOWLEDGMENTS

Authors are grateful to J-Ch. Hamilton for discussions in the initial stage of this work in our team. We also want to thank F.X Désert for useful discussions on the method and for corrections of this paper. The Healpix package (Gorski et al. 1998) was used extensively .

REFERENCES

Amblard A., Hamilton J. C., 2004, A&A, **417**, 1189
Ansari R. *et al.*, 2003, MNRAS, **343**, 552
Bennett C. L. *et al.*, 2003, ApJS, **148**, 97
Benoît A. *et al.*, 2003, A&A, **399**, L19
Benoît A. *et al.*, 2003, A&A, **399**, L25
Bond J.R., Jaffe A.H., Knox L., 1998, Phys. Rev. D, **57**, 2117.
Borrill J., 1999a, Phys. Rev. D, **59**, 27302.
Borrill J., 1999b, in EC-TMR Conf. Proc. 476, 3K Cosmology, eds. L. Maiani, F. Melchiorri and N. Vittorio, Woodbury AIP, 277.
Challinor A.D. *et al.*, 2002, MNRAS, **331**, 994.
Chon G. *et al.*, 2004, MNRAS, , **350**, 914
Delabrouille J., Cardoso J.-F., Patanchon G., 2003, MNRAS, **346**, 1089
Doran M., 2003, `arXiv:astro-ph/0302138`.
Douspis M., Bartlett J.G., Blanchard A. and Le Dour M., 2001, A&A, **368**, 1
Efstathiou G., 2004, MNRAS, **349**, 603
Fosalba P. *et al.*, 2002, Phys. Rev. D, **65**, 63003
Gorski K.M., Hivon E. & Wandelt B. D., 1998, Proceed. of the MPA/ESO Conf. on Evolution of Large-Scale Structure: from Recombination to Garching, 2-7 August 1998, eds. A.J. Banday, R.K. Sheth and L. Da Costa, `astro-ph/9812350`, http://www.eso.org/science/healpix
Grainge K. *et al.*, 2003, MNRAS, **341**, L23
Halverson N.W. *et al.*, 2002, ApJ, **568**, 38
Hansen F., Górski K. M., Hivon E., 2002, MNRAS, **336**, 1304
Hansen F., Górski K. M., 2003, MNRAS, **343**, 559
Hinshaw G. *et al.*, 2003, ApJS, **148**, 135
Hivon E. *et al.*, 2002, ApJ, **567**, 2
Hu W., Spergel D.N., White M., 1997, Phys. Rev. D, **55**, 3288
Jaffe A.H. *et al.*, 2003, New Astronomy Review, **47**, 727
Kuo C.L. *et al.*, 2004, ApJ, **600**, 32
Lewis A., Bridle S., 2002, Phys. Rev. D, **66**, 103511
Lewis A., Challinor A., Lasenby A., 2000, ApJ, **538**, 473
Liddle A.R., Lyth D.H., 2000, *Cosmological Inflation and Large-Scale Structure*, Cambridge University Press, Cambridge.
Linde A., Sasaki M., Tanaka T., 1999, Phys. Rev. D, **59**, 123522
Mitra S., Sengupta A. S., Souradeep T., 2004, Phys. Rev. D, accepted, `astro-ph/0405406`.
Page L. *et al.*, 2003, ApJS, **148**, 39
Peebles P.J.E., 1973, ApJ, **185**, 431
Peebles P.J.E., Hauser M.G., 1974, ApJS, **28**, 19.
Ruhl J.E. *et al.*, 2003, ApJ, **599**, 786
Schlegel D., Finkbeiner D., Davis M., 1998, ApJ, **500**, 525
Seljak U., Zaldarriaga M., 1996, ApJ, **469**, 437
Sievers J.L. *et al.*, 2003, ApJ, **591**, 599
Souradeep T., Ratra B., 2001, ApJ, **560**, 28
Szapudi I. *et al.*, 2001, ApJ, **548**, L115
Tegmark M., 1997, Phys. Rev. D, **55**, 5895.
Tegmark M., de Oliveira-Costa A., 2001, Phys. Rev. D, **64**, 63001.
Tristram M., Hamilton J-Ch., Macías-Peréz J.F., Renault C., 2004, Phys. Rev. D, 69, 123008
Tristram M., Patanchon G., Macías-Peréz J.F. *et al.*, 2005, A&A, submitted, `astro-ph/0411633`
van Leeuwen F. *et al.*, 2002, MNRAS, **331**, 975.
Varshalovich D.A., Moskalev A.N., Khersonoskii V.K., 1988, *Quantum theory of Angular Momentum*, World Scientific, Singapore.
Verde L. *et al.*, 2003, ApJS, **148**, 195
Wandelt B. D., Hivon E., Gorski K. M., 2001, Phys. Rev. D, **64**, 083003
Wandelt B. D., Gorski K. M., 2001, Phys. Rev. D, **63**, 123002
Wu J.H.P. *et al.*, 2000, ApJS, **132**, 1
Zaldarriaga M., Seljak U., Bertschinger, E., 1998, ApJ, **494**, 491
Zaldarriaga M., Seljak U., 2000, ApJS, **129**, 431

APPENDIX A: CORRELATION MATRIX

In this appendix we describe in details the calculation of the cross-correlation matrix $\Xi_{\ell\ell'}^{AB,CD}$ under the hypothesis of large sky coverage which leads to

$$\Xi_{\ell\ell'}^{AB,CD} \equiv \left\langle \Delta C_\ell^{AB} \Delta C_{\ell'}^{CD\,*} \right\rangle \tag{A1}$$

$$= \mathcal{M}_{\ell\ell_1}^{AB\,-1} \left\langle \Delta D_{\ell_1}^{AB} \Delta D_{\ell_2}^{CD\,*} \right\rangle (\mathcal{M}_{\ell'\ell_2}^{CD\,-1})^T \text{ where } \Delta X = \hat{X} - \langle X \rangle \tag{A2}$$

Let us remind that for Gaussian distributed variables x_i with variance $\langle x_i x_j \rangle = \sigma_{ij}^2$ the quadri-variance is given by

$$\begin{aligned} \langle x_i x_j x_k x_l \rangle &= \langle x_i x_j \rangle \langle x_k x_l \rangle + \langle x_i x_k \rangle \langle x_j x_l \rangle + \langle x_i x_l \rangle \langle x_j x_k \rangle \\ &= \sigma_{ij}^2 \sigma_{kl}^2 + \sigma_{ik}^2 \sigma_{jl}^2 + \sigma_{il}^2 \sigma_{jk}^2 \end{aligned} \tag{A3}$$

Using Eq A3, the main term of the cross-correlation matrix in Eq. A2 reads

$$\begin{aligned} \left\langle \widehat{D_{\ell_1}^{AB}} \widehat{D_{\ell_2}^{CD}}^{\,*} \right\rangle &= \frac{1}{(2\ell_1+1)(2\ell_2+1)} \sum_{m_1 m_2} \left\langle d_{\ell_1 m_1}^A d_{\ell_1 m_1}^{B*} d_{\ell_2 m_2}^{C*} d_{\ell_2 m_2}^D \right\rangle \\ &= \sum_{m_1 m_2} \frac{\left\langle d_{\ell_1 m_1}^A d_{\ell_1 m_1}^{B*} \right\rangle \left\langle d_{\ell_2 m_2}^{C*} d_{\ell_2 m_2}^D \right\rangle + \left\langle d_{\ell_1 m_1}^A d_{\ell_1 m_1}^{C*} \right\rangle \left\langle d_{\ell_1 m_1}^{B*} d_{\ell_2 m_2}^D \right\rangle + \left\langle d_{\ell_1 m_1}^A d_{\ell_2 m_2}^D \right\rangle \left\langle d_{\ell_1 m_1}^{B*} d_{\ell_2 m_2}^{C*} \right\rangle}{(2\ell_1+1)(2\ell_2+1)} \\ &= D_{l1}^{AB} D_{l2}^{CD} + \frac{1}{(2l1+1)(2l2+1)} \sum_{m_1 m_2} \left[\left\langle d_{l1 m_1}^A d_{l2 m_2}^{C*} \right\rangle \left\langle d_{l1 m_1}^{B*} d_{l2 m_2}^D \right\rangle + \left\langle d_{l1 m_1}^A d_{l2 m_2}^D \right\rangle \left\langle d_{l1 m_1}^{B*} d_{l2 m_2}^{C*} \right\rangle \right] \end{aligned}$$

where $d_{\ell m}$ are the coefficients of the spherical harmonic decomposition of the masked sky map such that

$$d_{\ell m} = \sum_{l1 m_1} a_{l1 m_1} K_{\ell m l1 m_1} \tag{A4}$$

with

$$K_{\ell_1 m_1 \ell_2 m_2} = \sum_i w_i \Omega_i Y_{\ell_1 m_1}(\theta_i) Y_{\ell_2 m_2}^*(\theta_i) \tag{A5}$$

$$= \sum_{\ell_3 m_3} (-1)^{m_2} w_{\ell_3 m_3} \left(\frac{(2\ell_1+1)(2\ell_2+1)(2\ell_3+1)}{4\pi} \right)^{1/2} \begin{pmatrix} \ell_1 & \ell_2 & \ell_3 \\ 0 & 0 & 0 \end{pmatrix} \begin{pmatrix} \ell_1 & \ell_2 & \ell_3 \\ m_1 & -m_2 & m_3 \end{pmatrix} \tag{A6}$$

Ω_i is the area of pixel i. w_i represents the mask applied to the sky map and $w_{\ell m}$ the coefficients of the spherical harmonic decomposition of the mask

$$w_{\ell m} = \sum_i w_i \Omega_i Y_{\ell m}(\theta_i). \tag{A7}$$

Thus, the cross-correlation matrix can be simply written as follows

$$\left\langle \Delta D_{l1}^{AB} \Delta D_{l2}^{CD\,*} \right\rangle = \frac{1}{(2l1+1)(2l2+1)} \sum_{m_1 m_2} \left[\left\langle d_{l1 m_1}^A d_{l2 m_2}^{C*} \right\rangle \left\langle d_{l1 m_1}^{B*} d_{l2 m_2}^D \right\rangle + \left\langle d_{l1 m_1}^A d_{l2 m_2}^D \right\rangle \left\langle d_{l1 m_1}^{B*} d_{l2 m_2}^{C*} \right\rangle \right] \tag{A8}$$

Let us develop each of the terms in Eq. A8, using $E_\ell = p_\ell B_\ell \sqrt{F_\ell}$

$$\begin{aligned} \left\langle d_{\ell m}^X d_{\ell' m'}^{Y*} \right\rangle &= \sum_{\ell_1 m_1} \sum_{\ell_2 m_2} \left\langle a_{\ell_1 m_1}^X a_{\ell_2 m_2}^{Y*} \right\rangle E_{l1}^X E_{l2}^Y K_{\ell m \ell_1 m_1}^X K_{\ell' m' \ell_2 m_2}^{Y*} \\ &= \sum_{\ell_1 m_1} C_{\ell_1}^{XY} E_{l1}^X E_{l1}^Y K_{\ell m \ell_1 m_1}^X K_{\ell_1 m_1 \ell' m'}^Y \\ &= \sum_{\ell_1 m_1} C_{\ell_1}^{XY} E_{l1}^X E_{l1}^Y \sum_{ij} w_i^X w_j^Y \Omega_i \Omega_j Y_{\ell m}(\theta_i) Y_{\ell_1 m_1}^*(\theta_i) Y_{\ell' m'}^*(\theta_j) Y_{\ell_1 m_1}(\theta_j) \end{aligned}$$

Assuming a large sky coverage (Efstathiou 2004) we can replace $C_{\ell_1}^{XY}$ by C_ℓ^{XY} and then, applying the completeness relation for spherical harmonics $\sum_{\ell m} Y_{\ell m}(\theta_i) Y_{\ell m}^*(\theta_j) = \frac{1}{\Omega_i} \delta(\theta_i - \theta_j)$, we obtain

$$\begin{aligned} \left\langle d_{\ell m}^X d_{\ell' m'}^{Y*} \right\rangle &= C_\ell^{XY} E_\ell^X E_\ell^Y \sum_i \left(w_i^X w_i^Y \right) \Omega_i Y_{\ell m}(\theta_i) Y_{\ell' m'}^*(\theta_i) \\ &= C_\ell^{XY} E_\ell^X E_\ell^Y K_{\ell m \ell' m'}^{(2)\,XY} \end{aligned} \tag{A9}$$

Thus, under the above hypothesis Eq. A8 reads

$$\left\langle \Delta D_{l1}^{AB} \Delta D_{l2}^{CD\,*} \right\rangle = \frac{E_{l1}^{A} E_{l1}^{C} E_{l2}^{B} E_{l2}^{D}}{(2l1+1)(2l2+1)} \sum_{m_1 m_2} \left[K^{(2)\,AC}_{l1m_1 l2m_2} K^{(2)\,BD}_{l1m_1 l2m_2} C_{l1}^{AC} C_{l2}^{BD} + K^{(2)\,AD}_{l1m_1 l2m_2} K^{(2)\,BC}_{l1m_1 l2m_2} C_{l1}^{AD} C_{l2}^{BC} \right] \tag{A10}$$

The above expression is equivalent to that for the coupling matrix $M_{\ell\ell'}$ presented in Hivon et al. 2002 and can be simplified as follows

$$\begin{aligned} \sum_{mm'} K^{(2)\,AC}_{\ell m \ell' m'} K^{(2)\,BD}_{\ell m \ell' m'} &= \sum_{mm'} \sum_{\ell_1 m_1} \sum_{\ell_2 m_2} w^{AC}_{\ell_1 m_1} w^{BD}_{\ell_2 m_2} \frac{(2\ell+1)(2\ell'+1)}{4\pi} \left((2\ell_1+1)(2\ell_2+1)\right)^{1/2} (-1)^{m_1+m_2} \\ &\quad \begin{pmatrix} \ell & \ell' & \ell_1 \\ 0 & 0 & 0 \end{pmatrix} \begin{pmatrix} \ell & \ell' & \ell_2 \\ 0 & 0 & 0 \end{pmatrix} \begin{pmatrix} \ell & \ell' & \ell_1 \\ m & -m' & -m_1 \end{pmatrix} \begin{pmatrix} \ell & \ell' & \ell_2 \\ m & -m' & -m_2 \end{pmatrix} \\ &= (2\ell+1) M^{(2)}_{\ell\ell'} \left(W^{AC,BD} \right) \end{aligned} \tag{A11}$$

where $M^{(2)}$ is the quadratic coupling kernel matrix

$$M^{(2)}_{\ell_1 \ell_2} \left(W^{AB,CD} \right) = (2\ell_2+1) \sum_{\ell_3} \frac{(2\ell_3+1)}{4\pi} W^{AB,CD}_{\ell_3} \begin{pmatrix} \ell_1 & \ell_2 & \ell_3 \\ 0 & 0 & 0 \end{pmatrix}^2 \tag{A12}$$

associated to the cross-power spectrum of the products of the masks $w_i^{XY} = w_i^X * w_i^Y$ for each of the cross-power spectra AB et CD,

$$W^{AB,CD} = \frac{1}{2\ell+1} \sum_m w^{AB}_{\ell m} w^{CD*}_{\ell m}$$

Replacing A11 in A10 we obtain the following expression

$$\left\langle \Delta D_{\ell_1}^{AB} \Delta D_{\ell_2}^{CD\,*} \right\rangle = \frac{E_{l1}^{A} E_{l1}^{C} E_{l2}^{B} E_{l2}^{D}}{2\ell_2+1} \left[M^{(2)}_{\ell_1\ell_2} \left(W^{AC,BD} \right) C_{\ell_1}^{AC} C_{\ell_2}^{BD} + M^{(2)}_{\ell_1\ell_2} \left(W^{AD,BC} \right) C_{\ell_1}^{AD} C_{\ell_2}^{BC} \right] \tag{A13}$$

and thus, using the same abreviation $\mathcal{M}^{(2)}_{l1l2} \left(W^{AC,BD} \right) = E_{l1}^{A} E_{l1}^{C} M^{(2)}_{\ell_1\ell_2} \left(W^{AC,BD} \right) E_{l2}^{B} E_{l2}^{D}$ the cross-correlation matrix reads,

$$\Xi^{AB,CD}_{\ell\ell'} = \mathcal{M}^{AB\,-1}_{\ell\ell_1} \left[\frac{\mathcal{M}^{(2)}_{\ell_1\ell_2} \left(W^{AC,BD} \right) C_{\ell_1}^{AC} C_{\ell_2}^{BD} + \mathcal{M}^{(2)}_{\ell_1\ell_2} \left(W^{AD,BC} \right) C_{\ell_1}^{AD} C_{\ell_2}^{BC}}{2\ell_2+1} \right] (\mathcal{M}^{CD\,-1}_{\ell'\ell_2})^T \tag{A14}$$